7

Microrheology of Complex Fluids

Laura J. Bonales, Armando Maestro, Ramón G. Rubio and Francisco Ortega
Departamento de Química Física I, Facultad de Química,
Universidad Complutense, Madrid
Spain

1. Introduction

Many of the diverse material properties of soft materials (polymer solutions, gels, filamentous proteins in cells, etc.) stem from their complex structures and dynamics with multiple characteristic length and time scales. A wide variety of technologies, from paints to foods, from oil recovery to processing of plastics, all heavily rely on the understanding of how complex fluids flow (Larson, 1999).

Rheological measurements on complex materials reveal viscoelastic responses which depend on the time scale at which the sample is probed. In order to characterize the rheological response one usually measures the shear or the Young modulus as a function of frequency by applying a small oscillatory strain of frequency ω. Typically, commercial rheometers probe frequencies up to tens of Hz, the upper range being limited by the onset of inertial effects, when the oscillatory strain wave decays appreciably before propagating throughout the entire sample. If the strain amplitude is small, the structure is not significantly deformed and the material remains in equilibrium; in this case the affine deformation of the material controls the measured stress, and the time-dependent stress is linearly proportional to the strain (Riande et al., 2000).

Even though standard rheological measurements have been very useful in characterizing soft materials and complex fluids (e.g. colloidal suspensions, polymer solutions and gels, emulsions, and surfactant solutions), they are not always well suited for all systems because milliliter samples are needed thus precluding the study of rare or precious materials, including many biological samples that are difficult to obtain in large quantities. Moreover, conventional rheometers provide an average measurement of the bulk response, and do not allow for local measurements in inhomogeneous systems. To address these issues, a new methodology, microrheology, has emerged that allows to probe the material response on micrometer length scales with microliter sample volumes. Microrheology does not correspond to a specific experimental technique, but rather a number of approaches that attempt to overcome some limitations of traditional bulk rheology (Squires & Mason, 2010; Wilson & Poon, 2011). Advantages over macrorheology include a significantly higher range of frequencies available without time-temperature superposition (Riande et al., 2000), the capability of measuring material inhomogeneities that are inaccessible to macrorheological methods, and rapid thermal and chemical homogeneization that allow the transient rheology of evolving systems to be studied (Ou-Yang & Wei, 2010). Microrheology methods typically use embedded micron-sized probes to locally deform the sample, thus allowing one to use this type of rheology on very small volumes, of the order of a microliter. Macro-

and microrheology probe different aspects of the material: the former makes measurements over extremely long (macroscopic) length scales using a viscometric flow field, whereas the latter effectively measures material properties on the scale of the probe itself (Squires & Mason, 2010; Breedveld & Pine, 2003). As the probe increases in size, one might expect that micro- and macrorheology would converge, however, as it has been suggested, it is possible that macro- and microrheology techniques do not probe exactly the same physical properties because - even in the continuum (large probe) limit - one experiment uses a viscometric flow whereas the other does not (Kahir & Brady, 2005; Lee et al., 2010; Schmidt et al., 2000; Oppong & de Bruyn, 2010).

One can distinguish two main families of microrheological experiments: One type of experiments focuses on the object itself; for example, the study of motor proteins aims at understanding the mechanical motions of the protein associated with enzymatic activities on the molecular level (Ou-Yang & Wei, 2010). The other type of experiment aims at understanding the local environment of the probe by observing changes in its random movements (Crocker & Grier, 1996; MacKintosh & Schmidt, 1999). Fundamentally different from relaxation kinetics, microrheology measures spontaneous thermal fluctuations without introducing major external perturbations into the systems being investigated. Other well-established methods in this family are dynamic light scattering (Dasgupta et al., 2002; Alexander & Dalgleish, 2007; Tassieri et al. 2010), and fluorescence correlation spectroscopy (Borsali & Pecora, 2008; Wöll et al., 2009). With recent advancement in spatial and temporal resolution to subnanometer and submillisecond, particle tracking experiments are now applicable to study of macromolecules (Pan et al., 2009) and intracellular components such as cytoskeletal networks (Cicuta & Donald, 2007). Detailed descriptions of the methods and applications of microrheology to the study of bulk systems have been given in review articles published in recent years (Crocker & Grier 1996; MacKintosh & Schmidt, 1999; Mukhopadhyay & Granick, 2001; Waigh, 2005; Gardel et al., 2005; Cicuta & Donald, 2007).

Interfaces play a dominant role in the behavior of many complex fluids. Interfacial rheology has been found to be a key factor in the stability of foams and emulsions, compatibilization of polymer blends, flotation technology, fusion of vesicles, etc. (Langevin, 2000). Also, proteins, lipids, phase-separated domains, and other membrane-bound objects diffuse in the plane of an interface (Cicuta et al., 2007). Particle-laden interfaces have attracted much attention in recent years because of the tendency of colloidal particles to become (almost irreversibly) trapped at interfaces and their behavior once there has lead to their use in a wide variety of systems including drug delivery, stabilization of foams and emulsions, froth, flotation, or ice cream production. There still is a need to understand the colloidal interactions to have control over the structure and therefore the properties of the particle assemblies formed, specially because it has been pointed out that the interactions of the particles at interfaces are far more complex than in the bulk (Binks & Horozov, 2006; Bonales et al., 2011). In recent years books and reviews of particles at liquid interfaces have been published (Kralchewski & Nagayama, 2001). The dynamic properties of particle-laden interfaces are strongly influenced by direct interparticle forces (capillary, steric, electrostatic, van der Waals, etc.) and complicated hydrodynamic interactions mediated by the surrounding fluid. At macroscopic scales, the rheological properties of particle-laden fluid interfaces can be viewed as those of a liquid-liquid interface with some effective surface viscoelastic properties described by effective shear and compressional complex viscoelastic moduli.

A significant fact is that for the simplest fluid-fluid interface, different dynamic modes have to be taken into account: the capillary (out of plane) mode, and the in-plane mode, which

contains dilational (or extensional) and shear contributions. For more complex interfaces, such as thicker ones, other dynamic modes (bending, splaying) have to be considered (Miller & Liggieri, 2009). Moreover, the coupling of the abovementioned modes with adsorption/desorption kinetics may be very relevant for interfaces that contain soluble or partially soluble surfactants, polymers or proteins (Miller & Liggieri, 2009; Muñoz et al., 2000; Díez-Pascual et al. 2007). In the case of surface shear rheology, most of the information available has been obtained using macroscopic interfacial rheometers which in many cases work at low Boussinesq numbers (Barentin et al., 2000; Gavranovic et. al., 2005; Miller & Liggieri, 2009; Maestro et al., 2011.a). Microrheology has been foreseen as a powerful method to study the dynamics of interfaces. In spite that the measurement of diffusion coefficients of particles attached to the interface is relatively straightforward with modern microrheological techniques, many authors have relied on hydrodynamic models of the viscoelastic surroundings traced by the particles in order to obtain variables such as interfacial elasticity or shear viscosity. The more complex the structure of the interface the stronger are the assumptions of the model, and therefore it is more difficult to check their validity. In the present work we will briefly review modern microrheology experimental techniques, and some of the recent results obtained for bulk and interfacial systems. Finally, we will summarize the theoretical models available for calculating the shear microviscosity of fluid monolayers from particle tracking experiments, and discuss the results for some systems.

2. Experimental techniques

For studying the viscoelasticity of the probe environment there are two broad types of experimental methods: active methods, which involve probe manipulation, and passive methods, that relay on thermal fluctuations to induce motion of the probes. Because thermal driving force is small, no sample deformation occurs that exceeds equilibrium thermal fluctuations. This virtually guarantees that only the linear viscoelastic response of the embedding medium is probed (Waigh, 2005). On the contrary, active methods allow the nonlinear response to be inferred from the relationship between driving force and probe velocity, in such cases the microstructure itself can be deformed significantly so that the material response differs from the linear case (Squires, 2008). As a consequence, passive techniques are typically more useful for measuring low values of predominantly viscous moduli, whereas active techniques can extend the measurable range to samples with significant elasticity modulus. Figure 1 shows the typical ranges of frequencies and shear moduli that can be studied with the different microrheological techniques.

2.1 Active techniques

2.1.1 Magnetic tweezers

This is the oldest implementation of an active microrheology technique, and it has been recently reviewed by Conroy (Conroy, 2008). A modern design has been described by Keller et al. (2001). The method combines the use of strong magnets to manipulate embedded super-paramagnetic or ferromagnetic particles, with video microscopy to measure the displacement of the particles upon application of constant or time-dependent forces. Strong magnetic fields are required to induce a magnetic dipole in the beads and magnetic field gradients are applied to produce a force. The force exerted is typically in the range of 10 pN to 10 nN depending on the experimental details (Keller et al. 2001). The spatial resolution is typically in the range of 10-20 nm, and the frequency range is 0.01 – 1000 Hz. Three modes

of operation are possible: a viscosimetry measurement after applying a constant force, a creep response experiment after applying a pulse excitation, and the measurement of the frequency dependent viscoelastic moduli in response to an oscillatory stress (Riande et al., 2000). This technique has been extensively applied to characterize the bulk viscoelasticity of systems of biological relevance (Wilson & Poon, 2011; Gardel et al., 2005). Moreover, real-time measurements of the local dynamics have also been reported for systems which change in response to external stimuli (Bausch et al., 2001), and rotational diffusion of the beads has also been used to characterize the viscosity of the surrounding fluid and to apply mechanical stresses directly to the cell surfaces receptors using ligand coated magnetic colloidal particles deposited onto the cell membrane (Fabry et al., 2001). Finally, this technique is well suited for the study of anisotropic systems by mapping the strain-field, and for studying interfaces (Lee et al., 2009). In recent years (Reynaert et al., 2008) have described a magnetically driven macrorheometer for studying interfacial shear viscosities in which one of the dimensions of the probe (a magnetic needle) is in the μm range. This has allowed the authors to work at rather high values of the Boussinesq number, which is one of the typical characteristics of the microrheology techniques.

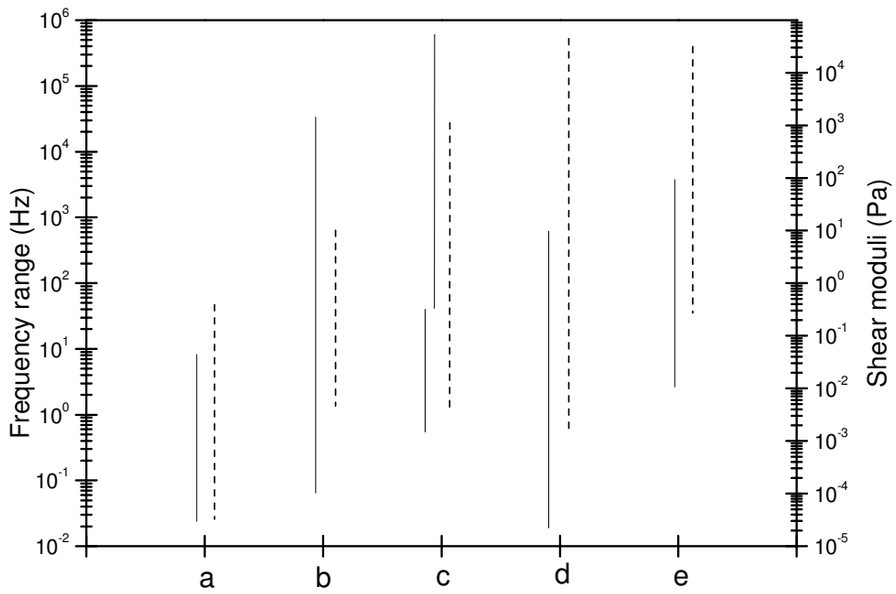

Fig. 1. Frequency and elasticity modulus range available to the different microrheological techniques. Continuous vertical represent the frequency range, and dashed arrows the range of shear moduli (G´, G´´) that are accessible to each technique. a)Video particle tracking. b) Optical Tweezers. c) Diffusing wave spectroscopy: upper line for transmission geometry, lower line for back geometry. d) Magnetic microrheology. e) Atomic Force Microscopy (AFM). Adapted from Waigh (2005).

2.1.2 Optical tweezers

This technique uses a highly focused laser beam to trap a colloidal particle, as a consequence of the momentum transfer associated with bending light. The most basic design of an optical tweezer is shown in Figure 2.a: A laser beam (usually in the IR range) is focused by a high-quality microscope (high numerical aperture objective) to a spot in a plane in the fluid.

Figure 2.b shows a detailed scheme of how an optical trap is created. Light carries a momentum, in the direction of propagation, that is proportional to its energy. Any change in the direction of light, by reflection or refraction, will result in a change of the momentum of the light. If an object bends the light, conservation momentum requires that the object must undergo an equal and opposite momentum change, which gives rise to a force acting on the subject. In a typical instrument the laser has a Gaussian intensity profile, thus the intensity at the center is higher than at the edges. When the light interacts with a bead, the sum of the forces acting on the particle can be split into two components: F_{sc}, the scattering force, pointing in the direction of the incident beam, and F_g, the gradient force, arising from the gradient of the Gaussian intensity profile and pointing in the plane perpendicular to the incident beam towards the center of the beam. F_g is a restoring force that pulls the bead into the center of the beam. If the contribution to F_{sc} of the refracted rays is larger than that of the reflected rays then a restoring force is also created along the beam direction and a stable trap exists. A detailed description of the theoretical basis and of modern experimental setups has been given in Refs. (Ou-Yang & Wei, 2010; Borsali & Pecora, 2008; Resnick, 2003) that also include a review of applications of optical and magnetic tweezers to problems of biophysical interest: ligand-receptor interactions, mechanical response of single chains of biopolymers, force spectroscopy of enzymes and membranes, molecular motors, and cell manipulation. A recent application of optical tweezers to study the non-linear mechanical response of red-blood cells is given by Yoon et al. (2008). Finally, optical tweezers are also suitable for the study of interfacial rheology (Steffen et al., 2001).

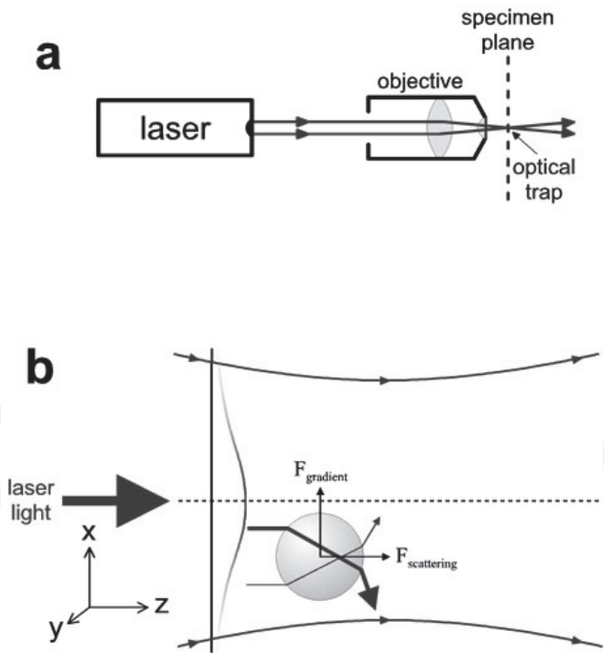

Fig. 2. a) Basic design of an optical tweezers instrument. b) Details of the physical principles leading to the optical trap.

2.2 Passive techniques

These techniques use the Brownian dynamics of embedded colloids to measure the rheology of the materials. Since passive methods use only the thermal energy of the beads, materials

must be sufficiently soft for the motion of the particles to be measure precisely. The resolution typically ranges from 0.1 to 10 nm and elastic modulus from 10 to 500 Pa can be measured with micron sized particles. Thermal fluctuations of particles in transparent bulk systems have traditionally been studied using light scattering techniques that allow one to measure the intensity correlation function from which the field correlation function $g_1(t)$ can be calculated, t being the time. For monodisperse particles $g_1(t)$ is directly related to the mean squared displacement of the particles, MSD, through

$$g_1(t) = \exp\left[-q^2 \langle \Delta r^2(t) \rangle / 6\right] \quad (1)$$

q being the scattering wave vector (Borsali & Pecora, 2008). Once $\langle \Delta r^2(t) \rangle$ is obtained, it is possible to calculate the real and imaginary components of the shear moduli, G′ and G″ (Oppong & de Bruyn, 2010).

2.2.1 Diffusion wave spectroscopy

Diffusion wave spectroscopy, DWS, allows measurements of multiple scattering media, and therefore non-transparent samples can be studied. The output of the technique allows to calculate $\langle \Delta r^2(t) \rangle$, and because of the multiple scattering all q-dependent information is lost as photons average over all possible angles, thus resulting only in two possible scattering geometries: transmission and backscattering. The frequency range of both geometries is complementary (see Figure 1) spanning from 0.1 Hz to 1MHz. For bulk polymer solutions and gels excellent agreement of the G′ and G″ values obtained by DWS and those obtained with conventional rheology has been found (Dasgupta et al., 2002; Dasgupta & Weitz, 2005). Even though these light scattering techniques are quite powerful tools for bulk microrheology, they have been scarcely used to probe the rheology of interfaces; in fact, as far as we know, only in old papers of Rice's group a set-up was described to measure dynamic light scattering of polymer monolayers using evanescent waves (Lin et al., 1993; Marcus et al., 1996).

2.2.2 Fluorescence correlation spectroscopy (FCS)

It is usually combined with optical microscopy, in particular confocal or two-photon microscopy. In these techniques light is focused on a sample and the fluorescence intensity fluctuations (due to diffusion, physical or chemical reactions, aggregations, etc.) can be measured in the form of a temporal correlation function. Similarly to what has been discussed in the light scattering technique, it is possible to obtain the MSD from the correlation function. In most experiments, Brownian motion drives the fluctuation of fluorescent-labeled molecules (or particles) within a well-defined element of the measurement cell. The samples have to be quite dilute, so that only few probes are within the focal spot (usually 1 – 100 molecules in one fL). Because of the tiny size of the confocal volume (approx. 0.2 fL), the measurements can be carried out in living cells or on cell membranes. In case that the interactions between two molecules wish to be studied, two options are available depending on their relative size. If their size is quite different, only one of them has to be labeled with a fluorescent dye (autocorrelation). If the diffusion coefficients of both molecules are similar, both have to be labeled with different dies (cross-correlation). A detailed description of FCS techniques and of the data analysis has been recently given by Riegler & Elson (2001). Recent problems to which FCS has been applied include: dynamics of rafts in membranes and vesicles, dynamics of supramolecular

complexes, proteins, polymers, blends and micelles, electrically induced microflows, diffusion of polyelectrolytes onto polymer surfaces, normal and confined diffusion of molecules and polymers, quantum dots blinking, dynamics of polymer networks, enzyme kinetics and structural heterogeneities in ionic liquids (Winkler, 2007; Heuf et al., 2007; Ries & Schwille, 2008; Cherdhirankorn et al., 2009; Wöll et al., 2009; Guo et al., 2011). The use of microscopes makes FCS suitable for the study of the dynamics of particles at interfaces. Moreover, contrary to particle tracking techniques, it is not necessary to "see" the particles, thus interfaces with nanometer sized particles can be studied (Riegler & Elson, 2001).

2.2.3 Particle tracking techniques

The main idea in particle tracking is to introduce onto the interface a few spherical particles of micrometer size and follow their trajectories (Brownian motion) using videomicroscopy. The trajectories of the particles, either in bulk or on surfaces, allow one to calculate the mean square displacement, which is related to the diffusion coefficient, D, and the dimensions, d, in which the translational motion takes place by

$$\left\langle \Delta r^2(t) \right\rangle = \left\langle \left[\vec{r}(t_0 - t) - \vec{r}(t_0) \right]^2 \right\rangle = 2dDt^{\alpha} \tag{2}$$

where the brackets indicate the average over all the particles tracked, and t_0 the initial time.
In case of diffusion in a purely viscous material or interface, α is equal to 1, and the usual linear relation is obtained between MSD and t. When the material or interface is viscoelastic, α becomes lower than 1 and this behavior is called sub-diffusive. It is worth noticing that sub-diffusivity can be found not only as a consequence of the elasticity of the material, but also due to particle interactions as concentration increases, an effect that is particularly important at interfaces. Anomalous diffusion is also found in many systems of biological interest where the Brownian motion of the particles is hindered by obstacles (Feder et al., 1996), or even constrained to defined regions (corralled motion) (Saxton & Jacobson, 1997).
The diffusion coefficient is related to the friction coefficient, f, by the Einstein relation

$$D = \frac{k_B T}{f} \tag{3}$$

In 3D Stokes law, $f=6\pi\eta a$, applies and for pure viscous fluids the shear viscosity, η, can be directly obtained from the diffusion coefficient of the probe particle of radius a at infinite dilution. The situation is much more complex in the case of fluid interfaces, and it will be discussed in more detail in the next section.
Figure 3 shows a sketch of a typical setup for particle tracking experiments. A CCD camera (typically 30 fps) is connected to a microscope that permits to image either the interface prepared onto a Langmuir trough, or a plane into a bulk fluid. The series of images are transferred to a computer to be analyzed to extract the trajectories of a set of particles. Figure 4.a shows typical results of MSD obtained for a 3D gel, combining DWS and particle tracking techniques which shows a very good agreement between both techniques, and illustrates the broad frequency range that can be explored. Figure 4.b shows a typical set of results for the MSD of a system of latex particles (1 μm of diameter) spread at the water/n-octane interface. The analysis of MSD within the linear range in terms of Eq. (2) allows to obtain D.

One of the experimental problems frequently found in particle tracking experiments is that the linear behavior of the MSD vs. t is relatively short. This may be due to poor statistics in calculating the average in Eq.(2), or to the existence of interactions between particles. As it will be discussed below, this may be a problem in calculating the shear modulus from the MSD. An additional experimental problem may be found when the interaction of the particles with the fluid surrounding them is very strong, which may lead to changes in its viscoelastic modulus, or when the samples are heterogeneous at the scale of particle size, a situation rather frequent in biological systems, e.g. cells (Konopka & Weisshaar, 2004), or gels (Alexander & Dalgleish, 2007), or solutions of rod-like polymers (Hasnain & Donald, 2006). In this case the so-called "two-point" correlation method is recommended (Chen et al., 2003). In this method the fluctuations of pairs of particles at a distance R_{ij} are measured for all the possible values of R_{ij} within the system. Vector displacements of individual particles are calculated as a function of lag time, t, and initial time, t_0.

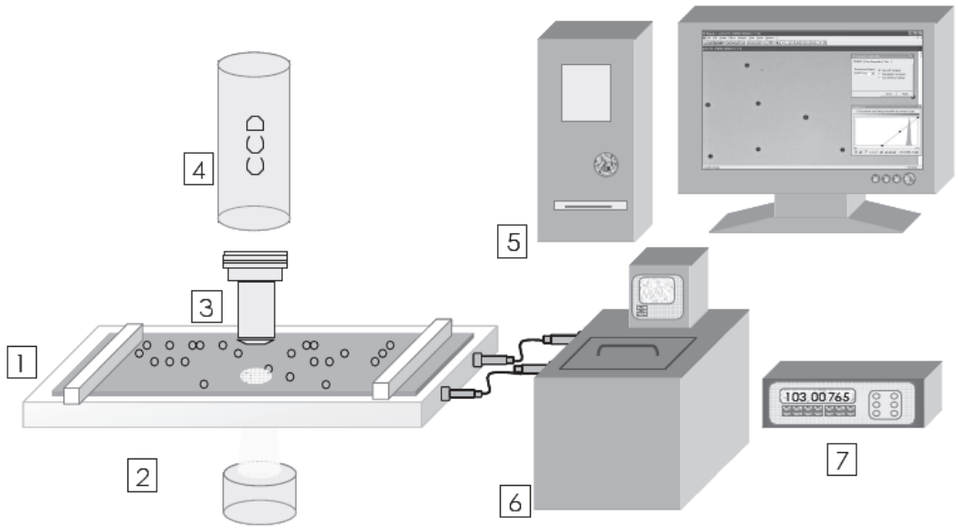

Fig. 3. Typical particle tracking setup for 2D microrheology experiments: 1: Langmuir trough; 2: illumination; 3: microscope objective; 4: CCD camera; 5: computer; 6: thermostat; 7: electronics for measuring the temperature and the surface pressure.

Then the ensemble averaged tensor product of the vector displacements is calculated (Chen et al., 2003):

$$D_{\alpha\beta}(r,\tau) = \left\langle \Delta r_{\alpha}^{i}(r,t)\Delta r_{\beta}^{j}(r,t)\delta\left[r - R_{ij}(t_0)\right]\right\rangle_{i\neq j,t} \tag{4}$$

where a and b are coordinate axes. The average corresponding to i = j represents the one-particle mean-squared displacement.

Two-point microrheology probes dynamics at different length scales larger than the particle radius, although it can be extrapolated to the particle's size thus giving the MSD (Liu et al., 2006). In fact it has been found that for R_{ij} close to the particle radius, the two-point MSD matches the tendency of the MSD obtained by tracking single particles. However, both sets of results are different for R_{ij}'s much larger than the particle diameter. This is a consequence of the fact that single particle tracking reflects both bulk and local rheologies, and therefore

the heterogeneities of the sample. Figure 5 shows a comparison of the MSD obtained by single particle and two-point tracking for a solution of entangled F-actin solutions at different length scales from 1 to 100 μm (Liu et al., 2006). Both methods agree when the particle size is of the same order than the scale of the inhomogeneities of the system when the particle probes the average structure. Otherwise, the two methods lead to different results. In general, quite good agreement is found between two-point tracking experiments and macroscopic rheology experiments.

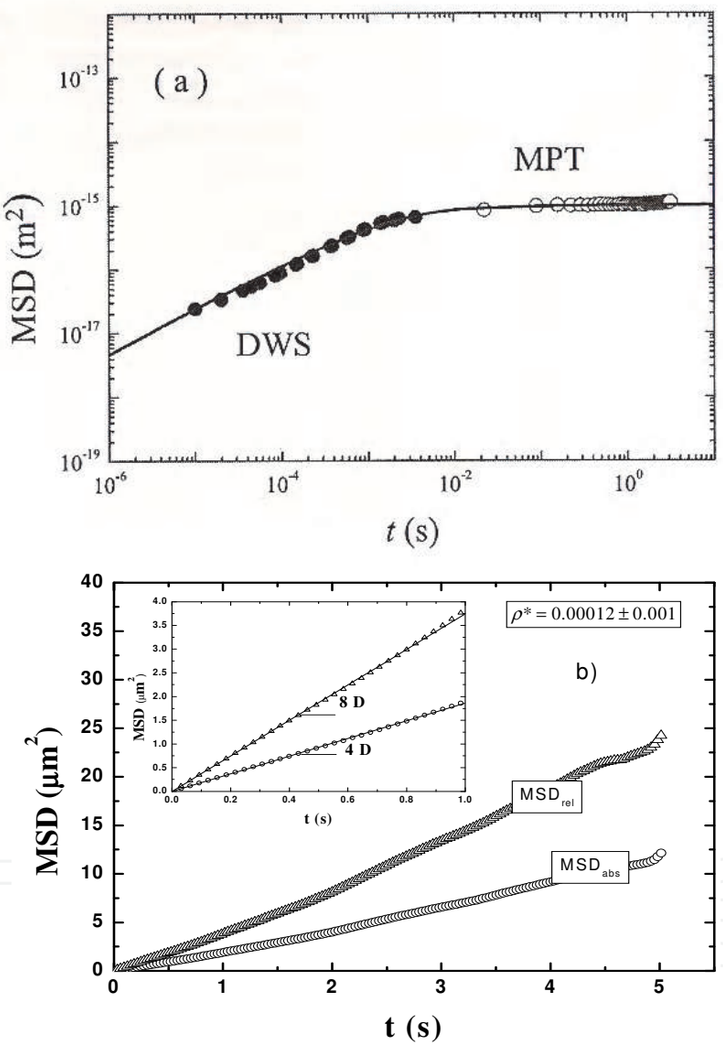

Fig. 4. a) Typical results of mean square displacement for a 3D gel made out of a polysaccharide in water [44]. Filled points are from DWS experiments, and open symbols are from particle tracking. The continuous line is an eye guide. b) Mean square displacement (MSD_{abs}), circles, and relative square displacement (MSD_{rel}), triangles, for latex particles at the water/n-octane interface. Experimental details: set of 300 latex particles of 1 μm of diameter, surface charge density: -5.8 mC·cm^{-2}, and reduced surface density, $\rho^*=1.2 \cdot 10^{-3}$ ($\rho^*=\rho a^2$), 25 ^{o}C. Figure 4.a is reproduced from Vincent et al. (2007). Inset corresponds to a smaller time interval.

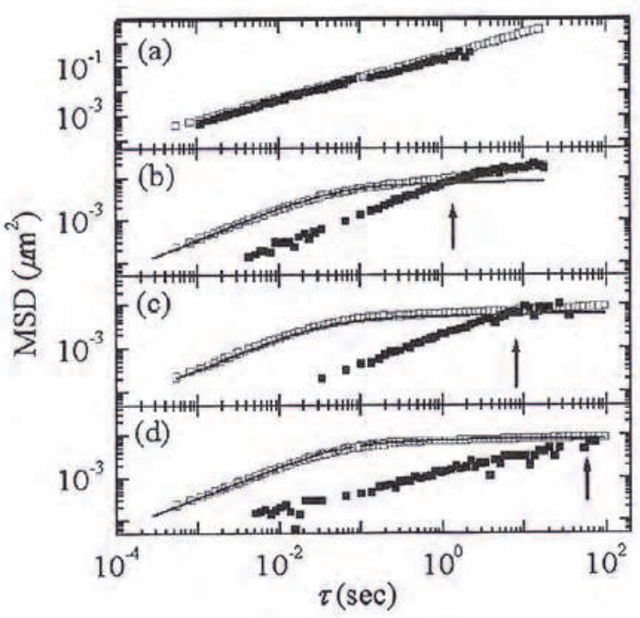

Fig. 5. Comparison of one-particle (open symbols) and two-particle (closed symbols) MSD for a solution of F-actin using particles of radius 0.42 μm. Different average actin filaments are used: a) 0.5 μm, b) 2 μm, c) 5 μm, d) 17 μm. Notice that when the scale of the inhomogeneities of the solution is similar to the particle size both methods lead to the same results. The figure is reproduced from Liu et al. (2006).

For the case in which the particles are embedded in a viscoelastic fluid, particle tracking experiments allow one to obtain the viscoelastic moduli of the fluids. Manson & Weitz (1995) first in an ad-hoc way, and later Levine & Lubensky (2000) in a more rigorous way, proposed a generalization of the Stokes-Einstein (GSE) equation:

$$\left\langle \Delta \tilde{r}^2(s) \right\rangle = \frac{2k_B T}{3\pi a s \tilde{G}(s)} \tag{5}$$

where $\tilde{G}(s)$ is the Laplace transform of the stress relaxation modulus, s is the Laplace frequency, and a is the radius of the particles. An alternative expression for the GSE equation can be written in the Fourier domain as:

$$G^*(\omega) = \frac{k_B T}{\pi a i \omega \Im\left\langle \Delta r^2(t) \right\rangle} \tag{6}$$

where $\Im$ represents a unilateral Fourier transform, which is effectively a Laplace transform generalized for a complex frequency iω. Different methods have been devised to obtain $\tilde{G}(s)$ from the experimental MSD including direct Laplace or Fourier transformations (Dasgupta et al., 2002; Evans et al., 2009), or analytical approximations (Mason, 2000; Wu & Dai, 2006). It must be stressed that the GSE equation is valid under the following approximations: (a) the medium around the sphere may be treated as a continuum material, which requires that the size of the particle be larger than any structural length scale of the

material, (b) no slip boundary conditions, (c) the fluid surrounding the sphere is incompressible, and (d) no inertial effects.

The application of the GSE is limited to a frequency range limited in the high frequency range by the appearance of inertial effects. The high frequency limit is imposed by the fact that the viscous penetration depth of the shear waves propagated by the particle motion must be larger than the particle size. The penetration depth is proportional to $(G^*/\rho\omega^2)^{1/2}$, where ρ is the density of the fluid surrounding the particles, and for micron-sized particles in water is of the order of 1 MHz. On the other hand, the lower limit is set by the time at which compressional modes become significant compared to the shear modes excited by the particle motion. An approximate value for the low frequency limit is given by

$$\omega_L \geq \frac{G'\xi^2}{\eta a} \tag{7}$$

ξ being the characteristic length scale of the elastic network in which the particles move. Again, for the same conditions mentioned above, the low-frequency limit is in the range of 0.1 to 10 Hz. Figure 6.a shows the frequency dependence of the shear modulus for a 3D gel using two passive techniques: DWS and particle tracking. As it can be observed the agreement is very good. It must be stressed that, in order to obtain reliable Laplace or Fourier transforms of the MSD, it is necessary to measure the particle trajectories over long t periods (minutes), which makes absolutely necessary to eliminate any collective drift in the system. Very recently Felderhof (2009) has presented an alternative method for calculating the shear complex modulus from the velocity autocorrelation function, VAF, that can be calculated from the particle trajectories. An experimental difficulty associated to this method is that the VAF decays very rapidly, and therefore it is difficult to obtain many experimental data in the decay region.

Under the same conditions assumed for the GSE equation, the creep compliance is directly related to the MSD by

$$J(t) = \frac{\pi a}{k_B T}\left\langle \Delta r^2(t) \right\rangle \tag{8}$$

Even though the GSE method has been applied to different bulk systems, few applications have been done for studying the complex shear modulus of interfaces and thin films (Wu & Dai, 2006; Prasad & Weeks, 2009; Maestro et al., 2011).

The two-point correlation method also provides information about the viscoelastic moduli of the fluid in which the particles are embedded. In effect, the ensemble averaged tensor product, Eq.(4), leads to (Chen et al., 2003)

$$\tilde{D}_{rr}(r,s) = \frac{k_B T}{2\pi r s \tilde{G}(s)}; \quad D_{\theta\theta} = D_{\phi\phi} = \frac{1}{2} D_{rr} \tag{9}$$

where $\tilde{D}_{rr}(r,s)$ is the Laplace transform of $D_{rr}(r,t)$ and the off-diagonal terms vanish. Figure 6.b compares the G′ and G″ results calculated for a solution of F-actin (MSD data shown in Figure 4) using one- and two-particle tracking methods. The results agree with those obtained by single-particle methods as far as the scale of the inhomogeneities is similar to the particle size, otherwise the single particle method is affected both by local and global

rheology. Notice that the results of the two-point technique agree with those obtained with conventional macroscopic rheometers.

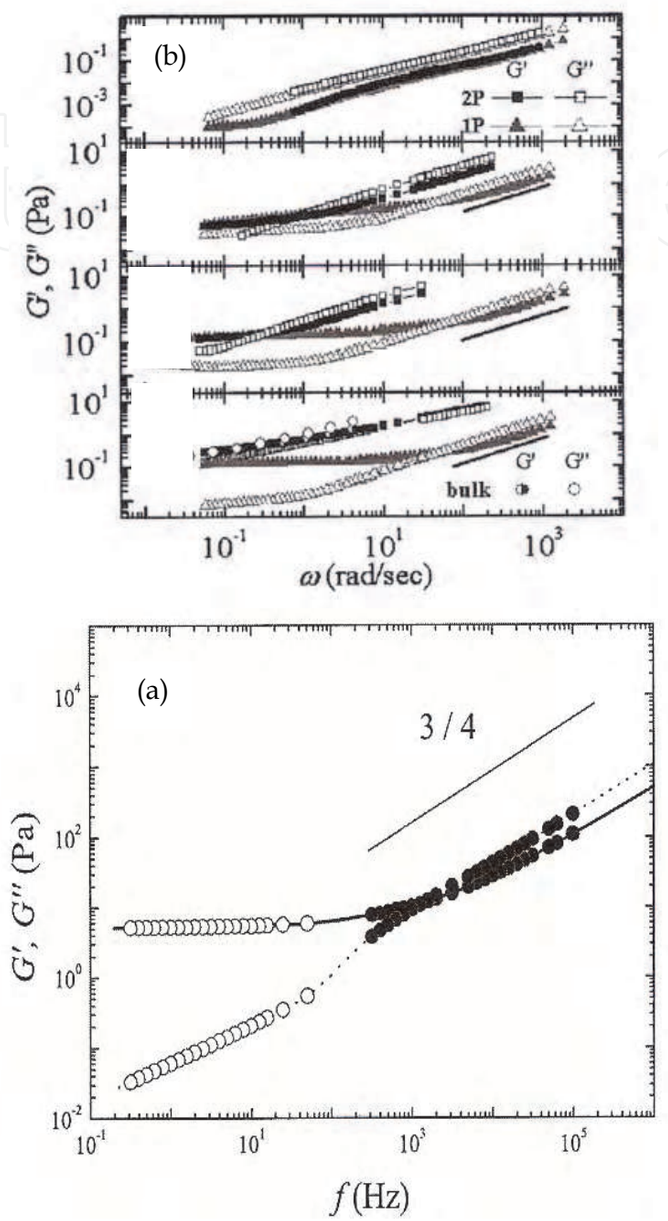

Fig. 6. Real and imaginary components calculated from the MSD shown in: a) the Figure 4.a, and b) Figure 5. Notice the good agreement between the results calculated from DWS (closed symbols) and single particle tracking (open symbols) in Figure 5.a. The solid and dotted lines are guides for G'and G" results, respectively. In Figure 6.b the open symbols refer to G", and the full ones to G'. Triangles correspond to single particle tracking and squares to two-particle tracking. Circles correspond to conventional macro-rheology. Figure 6.a was taken from Vincent et al. (2007) and Figure 6.b from Cherdhirankorn et al. (2009).

3. Dynamics of particles at interfaces

For using particle tracking techniques to get insight of the interfacial microrheology it is first necessary to study the diffusion of particles in the bare interface. For an inviscid interface the drag comes entirely from the upper and lower fluid phases (in the usual air-water interface only from the water subphase). The MSD of particles trapped at fluid interfaces depends on the surface concentration, and for very low surface concentration it is linear with time, thus the diffusion coefficients, D_0, can be easily obtained. However, for high surface concentrations, even below the threshold of aggregation or fluid-solid phase transitions (Bonales et al., 2011), the MSD is no longer linear with time, but shows a sub-diffusive behavior, MSD(t) ~ t^{α} with $\alpha<1$, hence D_0 must be obtained from the time dependence of the MSD in the limit of short times.

3.1 Shear micro-rheology of monolayers at fluid interfaces

In the case of particles trapped at interfaces Einstein's equation, Eq.(3), is still valid. However, one cannot calculate the friction coefficient using Stokes equation and directly substituting the interfacial shear viscosity. Instead, f is a function of the viscosities of the phases (η's), the geometry of the particle (the radius "a" for spheres), the contact angle between the probe particle and the interface (θ), etc. For a pure 2D system there is no solution for the slow viscous flow equations for steady translational motion of a sphere in a 2D fluid (Stokes paradox).

3.1.1 Motion of a disk in and incompressible membrane of arbitrary viscosity

Saffman & Delbrück (1975) and Hughes et al. (1981) have solved the problem of the motion of a thin disk immersed in a membrane of arbitrary viscosity, η_L separating two phases of viscosities η_1 and η_2. The height of the disk is assumed to be equal to the membrane thickness, h. They obtained the following expression for the translational mobility,

$$b_T = \frac{1}{f} = \frac{1}{4\pi(\eta_1+\eta_2)R\Lambda(\varepsilon)} \tag{10}$$

Where $\Lambda(\varepsilon)$ is non-linear function of ε, $\left[\varepsilon = \frac{R}{h}\left(\frac{\eta_1+\eta_2}{\eta_L}\right)\right]$. $\Lambda(\varepsilon)$ cannot be expressed analytically except for two limit cases,

$$\Lambda(\varepsilon) = \left\{\varepsilon\left(\ln\left(\frac{2}{\varepsilon}\right) - \gamma + \frac{4}{\pi}\varepsilon - \frac{1}{2}\varepsilon^2\ln\left(\frac{2}{\varepsilon}\right) + O(\varepsilon^2)\right)\right\}^{-1} \qquad \text{(Highly viscous membranes, e<1)}$$

$$\Lambda(\varepsilon) = \frac{2}{\pi} \qquad \text{(Low viscous membranes, } \varepsilon>1\text{)}$$

These works have been generalized by Stone & Adjari (1998) and by Barentin et al. (2000).

3.1.2 Danov's model for a sphere in a compressible surfactant layer

The above theories are limited to non protruding particles (or high membrane viscosities). In particle tracking experiments spherical particles are used that are partially immersed in both

fluid phases separating the interface. Danov et al. (1995) and Fischer et al. (2006) have made numerical calculations of the drag coefficient of spherical microparticles trapped at fluid-fluid interfaces. While Danov considered the interface as compressible, Fischer assumed that the interface is incompressible, both authors predicted the dynamics of the particles adsorbed on bare fluid interfaces, i.e. with no surfactant monolayers (the so-called the limit of cero surface viscosity). The predictions of their theories are different, and will be discussed in detail below. More recently, Reynaert et al. (2007) and Madivala et al. (2009) have studied the dynamics of spherical, weakly aggregated, and of non-spherical particles at interfaces, though using macroscopic rheometers.

Danov et al. (1995) have calculated the hydrodynamic drag force and the torque acting on a micro spherical particle trapped at the air-liquid interface (they consider the viscosity of air to be zero) interface, and moving parallel to it. This model was later extended by Dimova et al. (2000) and by Danov et al. (2000) to particles adsorbed to flat or curved (spherical) interfaces separating two fluids of non vanishing viscosity. The interface was modeled as a *compressible*, 2D fluid characterized by two dimensionless parameters K and E defined as $\mathrm{E} = \eta_{\mathrm{sh}}/(\eta \mathrm{a})$ and $\mathrm{K} = \eta_{\mathrm{d}}/(\eta \mathrm{a})$, being η_{sh} and η_d the surface shear and dilational viscosity respectively (Note that E is the inverse of ε used by Hughes). Danov et al. made the following assumptions: 1) The movement implies a low Reynolds number, thus they ignored any inertial term; 2) the moving particle is not affected by capillarity or electro-dipping; 3) the contact line does not move to respect to the particle surface, and 4) they considered E=K, i.e. the interface is compressible. With these assumptions they solved numerically the Navier-Stokes equation to obtain the values of the drag coefficient f as a function the contact angle and of E (or K). They presented their results in graphical form, and their results are reproduced in Figure 7.

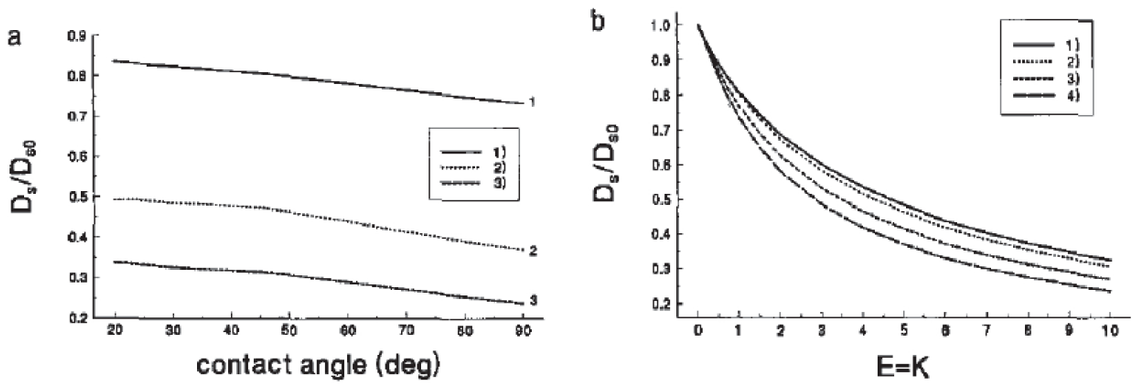

Fig. 7. Left: Effect of contact angle on the diffusion coefficient of a particle trapped at a fluid interface according to Danov's theory. D_{s0} is the diffusion coefficient for the bare interface. The different lines correspond to the following values of E (=K): 1) 0; 2) 1; 3) 5. Right: Effect of the surface to bulk shear viscosity on the diffusion coefficient. The different lines correspond to the following values of E (=K): 1) 0; 2) 1; 3) 5; 4) 10. Figures reproduced from Dimova et al. (2000).

These curves can be used to obtain the shear viscosity of compressible surfactant layer once one has obtained the diffusion coefficient from particle tracking experiments, D_0, for a free interface and in the presence of a surfactant layer. It must be stressed that, from a strict

theoretical point of view, the results presented by Danov are valid only in the limit E >>1, and for arbitrary values of the contact angle. Sickert & Rondelez (2003) were the first to applied Danov's ideas to obtain the surface shear viscosity by particle tracking using spherical microparticles trapped at the air-water interface, which was covered with Langmuir films. They have measured the surface viscosity of three monolayers formed by pentadecanoic acid (PDA), L-a-dipalmitoylphosphatidylcholine (DPPC) and N-palmitoyl-6-n-penicillanic acid (PPA) respectively. The values of the shear viscosities for PDA, DPPC and PPA reported were in the range of 1 to 11.10^{-10} $N \cdot s \cdot m^{-1}$ in the liquid expanded region of the monolayer. These values are beyond the range that can be reached by macroscopic mechanical methods, that usually have a lower limit in the range of 10^{-7} $N \cdot s \cdot m^{-1}$.
Fischer considered that a monolayer cannot be considered as compressible. Due to the presence of a surfactant, Marangoni forces (forces due to surface tension gradients) strongly suppress any motion at the surface that compress or expands the interface. Any gradient in the surface pressure is almost instantly compensated by the fast movement of the surfactant at the interface given a constant surface pressure, behaving thus as a incompressible monolayer (Fischer assumed that the velocity of the 2D surfactant diffusion is faster than the movement of the beads). The fact that the drag on a disk in a monolayer is that of an incompressible surface has been verified experimentally by Fischer (2004). In the case of Langmuir films of polymers, the monolayer could be considered as compressible or incompressible depending on the rate of the polymer dynamics at the interface compared to the velocity of the beads probes. Bonales et al. (2007) have calculated the shear viscosity of two polymer Langmuir films using Danov's theory, and compared these values with those obtained by canal viscosimetry. Video Particle tracking and Danov's theory were used by Maestro et al. (2011.a) to show the glass transition in Langmuir films. Figure 8 shows the results obtained for a monolayer of poly(4-hydroxystyrene) onto water. For all the monolayers reported by Bonales et al. (2007) and Maestro et al. (2011.b) the surface shear viscosity calculated from Danov's theory was lower than that measured with the macroscopic canal surface viscometer. Similar qualitative conclusions were reached at by Sickert et al. (2007) for monolayers of fatty acids and phospholipids in the liquid expanded region.

3.1.3 Fischer's theory for a sphere in a incompressible surfactant layer

Fischer et al. (2006) have numerically solved the problem of a sphere trapped at an interface with a contact angle θ moving in an *incompressible* surface. They showed that contributions due to Marangoni forces account for a significant part of the total drag. This effect becomes most pronounced in the limit of vanishing surface compressibility. In this limit the Marangoni effects are simply incorporated to the model by approximating the surface as incompressible. They solved the fluid dynamics equations for a 3D object moving in a monolayer of surface shear viscosity, η_s between two infinite viscous phases. The monolayer surface is assumed to be flat (no electrocapillary effects). Then the translational drag coefficient, $k_{T,}$, was expressed as a series expansion of the Boussinesq number, $B = \eta_s / \left((\eta_1 + \eta_2) \cdot a \right)$, a being the radius of the spherical particle:

$$k_T = k_T^0 + Bk_T^1 + O(B^2) \tag{11}$$

For B=0, and for an air-water interface (η_1, η_2=0), the numerical results for k_T are fitted with an accuracy of 3% by the formula,

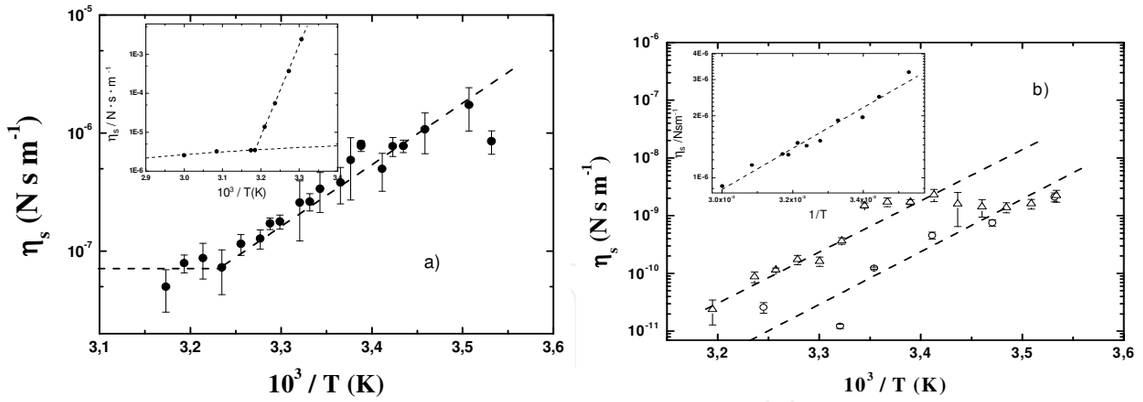

Fig. 8. Temperature dependence of the surface shear viscosity of a monolayer of poly(4-hydroxystyrene) at the air-water interface obtained by particle tracking (the insets show the corresponding values measured with a macroscopic canal viscometer. Left: experiments done at Π=8 mN·m^{-1}. Right: triangles correspond to Π=3 mN·m^{-1} and circles to Π=2 mN·m^{-1}. Notice that the results obtained by particle tracking are much smaller than those obtained with the canal viscometer. Data taken from Hilles et al. (2009).

$$k_T^0 \approx 6\pi\sqrt{\tanh\left(32\left(\frac{d}{R}+2\right)\Big/\left(9\pi^2\right)\right)} \tag{12}$$

where d is the distance from the apex of the bead to the plane of the interface (which defines the contact angle). Note that if d goes to infinity, $k_T^0 = 6\pi$, which is the correct theoretical value for a sphere in bulk (Stokes law). The translational drag in a half immersed sphere in a non viscous monolayer is $k_T^0 \approx 11$ which is about 25% higher than the drag on a sphere trapped at a free surface, $k_T = 3\pi$. This means that even in the absence of any appreciable surface viscosity the drag coefficient of an incompressible monolayer is higher than that of a free interface, and the data cannot be used to extract the surface shear viscosity using Danov's theory especially in the limit of low surface viscosities.
The numerical results for $k_T^{(1)}$ are fitted within an accuracy of 3% to,

$$k_T^{(1)} \approx \begin{cases} -4\ln\left(\frac{2}{\pi}\arctan\left(\frac{2}{3}\right)\right)\left(\frac{a^{3/2}}{(d+3a)^{3/2}}\right) & (d/a>0) \\ -4\ln\left(\frac{2}{\pi}\arctan\left(\frac{d+2a}{3a}\right)\right) & (d/a<0) \end{cases} \tag{13}$$

Sickert & Rondelez (2003) have introduced in an ad-hoc way the incompressibility effect in Danov's theory by renormalizing his master curve (Figure 7 above) by the empirical value of 1.2, and they have later reanalyzed their data by combining the Danov's and Fischer's theories (Sickert et al., 2007). First they used the value determined by Danov et al. (2000) for the resistance coefficient of a sphere at a clean, compressible surface and at the contact angle of their experiments (50^o). Afterwards, they used the predictions of Fischer et al. (2006) for a sphere in a surfactant monolayer (incompressible) with the contact angle corrected by the change in the surface tension, and in the case of E <<<1 (notice that this is the opposite E-limit than for the original Danov's theory),

$$\frac{D_0}{D_{\to 0}} = \frac{\xi_0^{(Danov)}(\theta)}{\xi^{(Fisher)}(\theta)} = \frac{\xi_0^{(Danov)}(\theta)}{k_T^0(\theta) + Ek_T^1(\theta)} \tag{14}$$

D_0 being the diffusion coefficient of the beads at a free surface (compressible), and $D_{\to 0}$ is the value of an incompressible monolayer which surface concentration is tending to zero. They found that this relation is not equal to 1 but to 0.84 for their systems and experimental conditions which confirms the observation of Barentin et al. (2000).

Figure 9 shows the friction coefficient for latex particles at the water-air interface obtained from particle tracking for polystyrene latex particles. It also shows the values calculated from Danov's and from Fischer's theories (notice that for the bare interface E = B =0). The figure clearly shows that both theories underestimate the experimental values over the whole θ range. An empirical factor of $\eta(\theta)_{exp}/\eta(\theta)_{Fisher}$ = 1.8±0.2 brings the calculated values in good agreement with the experiments at all the contact angle values. A similar situation was found for the water-n-octane interface.

The values of the shear viscosities calculated by Sickert & Rondelez (2003) by using the modified-Fisher theory are 2 or 3 times higher than the previous values. Sickert et al. (2007) also refers to a model developed by Stone which would be valid over the whole range of E, although only for a contact angle of 90º. Figure 10 shows clearly the large difference found between micro- and macrorheology for monolayers of poly(t-butyl acrylate) at the so-called Γ** surface concentration (Muñoz et al., 2000). The macrorheology results have been obtained using two different oscillatory rheometers. The huge difference cannot be attributed to specific interactions between the particles and the monolayer.

In effect, Figure 11 shows that the values obtained are the same for particles of rather different surface characteristics. Moreover, the values calculated from the modified-Fisher's theory or by direct application of the GSE equation lead to almost indistinguishable surface shear viscosities. It must be stressed that in all the cases the contact angle used is the experimentally measured using the gel-trapping technique described by Paunov et al.

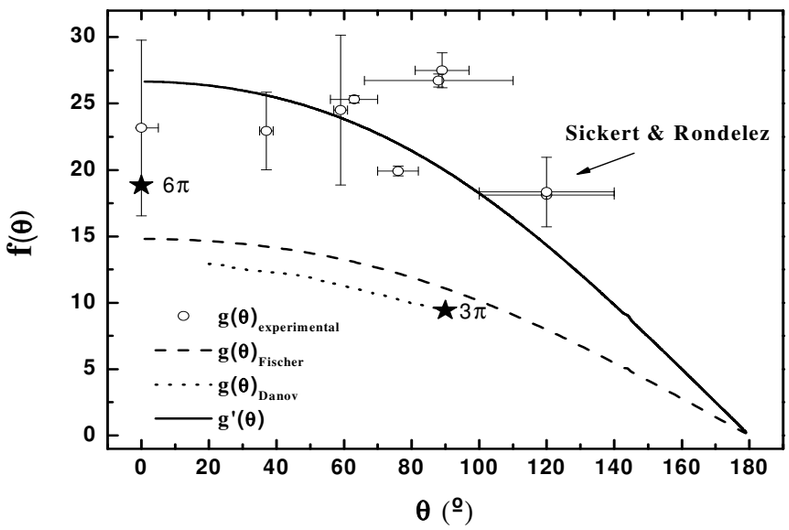

Fig. 9. Friction coefficients calculated from the experimental diffusion coefficients measured by particle tracking experiments (symbols), by Danov's theory (dotted line), by Fischer's theory (dashed line), and by the corrected Fischer's theory (continuous line).

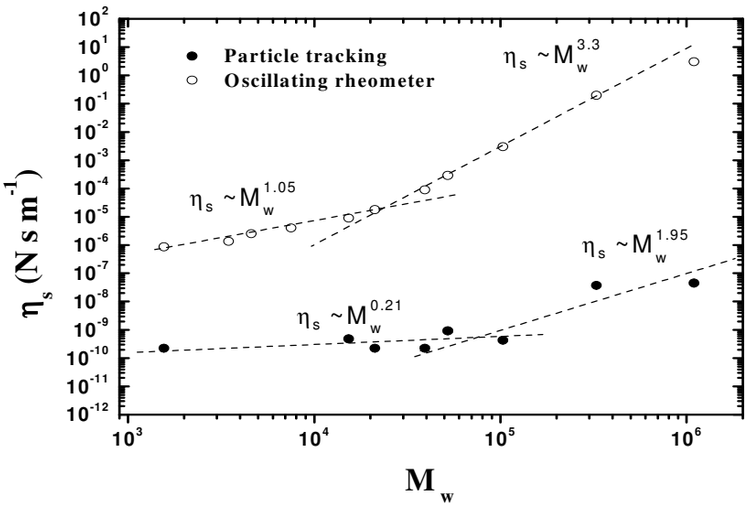

Fig. 10. Surface shear viscosity for monolayers of poly(t-butyl acrylate) as a function of the molecular weight and for a surface pressure of 16 mN m^{-1}. The lower curve corresponds to data obtained from particle tracking. The upper curve was obtained from conventional oscillatory rheometers.

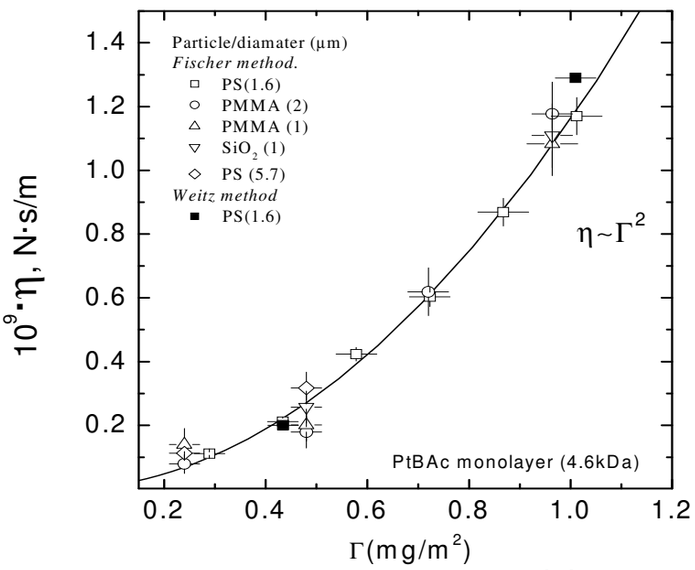

Fig. 11. Surface shear viscosity of a monolayer of poly(t-butyl acrylate) (molecular weight 4.6 kDa) measured by particle tracking. Different microparticles where used: poly(styrene) of 1.6 and 5.7 μm (stabilized by sulfonate groups); poly(methylmethacrylate) stabilized by Coulombic repulsions (PMMA1), or by steric repulsions (PMMA2); Silica particles stabilized by Coulombic repulsions. Empty symbols: the viscosities were calculated using Fischer theory. Full symbols: calculated by the GSE equation.

(2003). This discrepancy between micro- and macrorheology in the study of monolayers seems to be a rather general situation (Schmidt et al., 2000; Khair & Brady, 2005; Oppong & de Bruyn, 2010; Lee et al., 2010) and no clear theoretical answer has been found so far.

4. Conclusions

The set of microrheological techniques offer the possibility of studying the rheology of very small samples, of systems which are heterogeneous, and facilitate to measure the shear modulus over a broad frequency range. Particle tracking techniques are especially well suited for the study of the diffusion of microparticles either in the bulk or at fluid interfaces. Different types of mean squared displacements, MSD, (one-particle, two-particle) allow one to detect spatial heterogeneities in the samples. Even though good agreement has been found between micro- and macrorheology (at least when two-particle MSD is used) in bulk systems, the situation is still not clear for the case of fluid interfaces, where the shear surface microviscosity is much smaller than the one measured with conventional surface rheometers.

5. Acknowledgments

This work has been supported in part by MICIN under grant FIS2009-14008-C02-01, by ESA under grant FASES MAP-AO-00-052, and by U.E. under grant Marie-Curie-ITN "MULTIFLOW". L.J. Bonales and A. Maestro are grateful to MICINN for their Ph.D. fellowships. We are grateful to Th.M. Fisher, R. Miller and L. Liggieri for helpful discussions.

6. References

Alexander M., Dalgleish D.G., 2007, Diffusing wave spectroscopy of aggregating and gelling systems. *Curr. Opinion Colloid Interf. Sci.* 12 (4-5) 179-186, ISSN: 1359-0294

Barentin C., Muller, P., Ybert, C., Joanny J.-F., di Meglio J.-M., 2000, Shear viscosity of polymer and surfactant monolayers. *Eur. Phys. J. E.* 2 (2) 153-159, ISSN: 1292-8941

Bausch A.R., Hellerer U., Essler M., Aepfelbacher M., Sackmann E., 2001, Rapid stiffening of integrin receptor-actin linkages in endothelial cells stimulated with thrombin: A magnetic bead microrheometry study. *Biophys. J.* 80 (6) 2649-2657, ISSN: 0006-3495

Binks B., Horozov S., (Eds.), 2006, *Colloidal particles at liquid interfaces*. Cambridge Univ. Press, ISBN: 9780521848466, Cambridge.

Bonales L.J., Ritacco H., Rubio J.E.F., Rubio R.G., Monroy F., Ortega F., 2007. Dynamics in ultrathin films: Particle tracking microrheology of Langmuir monolayers. *Open Phys. Chem. J.* 1 (1) 25-32; ISSN: 1874-0677

Bonales L.J., Rubio J.E.F., Ritacco H., Vega C., Rubio R.G., Ortega F., 2011. Freezing transition and interaction potential in monolayers of microparticles at fluid interfaces. *Langmuir* 27 (7) 3391-3400, ISSN: 0743-7463.

Borsali R., Pecora R., (Eds.), 2008. *Soft-matter characterization.* Vol. 1., Springer, ISBN: 978-**1-**4020-8290-0, Berlin.

Breedveld V., Pine D.J., 2003, Microrheology as a tool for high-throughput screening. *J. Mater. Sci.* 38 (22), 4461-4470, ISSN: 002-2461

Chen D.T., Weeks E.R., Crocker J.C., Islam M.F., Verma R., Gruber J., Levine A.J., Lubensky T.C., Yodh A.G., 2003, Rheological microscopy. Local mechanical properties from microrheology. *Phys. Rev. Lett.* 90 (10) 108301, ISSN: 0031-9007

Cherdhirankorn T., Harmandaris V., Juhari A., Voudouris P., Fytas G., Kremer K., Koynov K., 2009, Fluorescence correlation spectroscopy study of molecular probe diffusion in polymer melts. *Macromolecules* 42 (13) 4858-4866, ISSN: 0024-9297

Cicuta P., Donald A.M., 2007, Microrheology: a review of the method and applications. *Soft Matter* 3 (12) 1449-1455, ISSN: 1744-683X

Cicuta P., Keller S.L., Veatch S.L., 2007, Diffusion of Liquid Domains in Lipid Bilayer Membranes , *J. Phys. Chem. B* 111 (13) 3328-3331, ISSN:1520-6106

Conroy R., 2008, Force spectroscopy with optical and magnetic tweezers. In *Handbook of molecular force spectroscopy*. Noy A. (Ed.), Springer, ISBN: 978-0-387-49987-1, Berlin.

Crocker J.C., Grier D.G., 1996, Methods of digital video microscopy for colloidal studies. *J. Colloid Interf. Sci.* 179 (1), 298-310, ISSN: 0021-9797

Danov K., Aust R., Durst F., Lange U. 1995. Influence of the surface viscosity on the hydrodynamic resistance and surface diffusivity of a large Brownian particle. *J. Colloid Int. Sci*., 175 (1), 36-45, ISSN: 0021-9797

Danov K.D., Dimova R., Pouligny B. 2000. Viscous drag of a solid sphere stradding a spherical or flat surface. *Physics of Fluids,* 12 (11) 2711-2722, ISSN: 0899-8213

Dasgupta B.R., Tee S.Y., Crocker J.C., Frisken B.J., Weitz D.A., 2002, Microrheology of polyethylene oxide using diffusing wave spectroscopy and single scattering. *Phys. Rev. E* 65 (5) 051505, ISSN: 1539-3755

Dasgupta B.R., Weitz D.A., 2005, Microrheology of cross-linked polyacrylamide networks. *Phys. Rev. E* 71 (2) 021504, ISSN: 1539-3755

Díez-Pascual A.M., Monroy F., Ortega F., Rubio R.G., Miller R., Noskov B.A., 2007, Adsorption of water-soluble polymers with surfactant character. Dilational viscoelasticity. *Langmuir* 23 (7) 3802-3808, ISSN: 0743-7463

Dimova R., Danov K., Pouligny B., Ivanov I.B. 2000. Drag of a solid particle trapped in a thin film or at an interface: Influence of surface viscosity and elasticity. *J. Colloid Interf. Sci*. 226 (1) 35-43, ISSN: 0021-9797

Evans R.M., Tassieri M., Auhl D., Waigh Th.A., 2009, Direct conversion of rheological compliance measurements into storage and loss moduli. *Phys. Rev. E* 80 (1) 012501, ISSN: 1539-3755

Fabry B., Maksym G.N., Butler J.P., Glogauer M., Navajas D., Fredberg JJ. 2001, Scaling the microrheology of living cells. *Phys. Rev. Lett.* 87 (14) 148102, ISSN: 0031-9007

Feder T.J., Brust-Mascher I., Slattery J.P., Barid B., Webb W.W., 1996, Constrained diffusion or immobile fraction on cell surfaces: A new interpretation. *Biophys. J.* 70 (6) 2767-2773, ISSN: 0006-3495

Felderhof B.U., 2009, Estimating the viscoelastic moduli of a complex fluid from observation of Brownian motion. *J. Chem. Phys.* 131 (16) 164904, ISSN: 0021-9606

Fischer Th.M. 2004. Comment on "Shear viscosity of Langmuir Monolayers in the Low Density Limit". *Phys. Rev. Lett.* 92 (13) 139603, ISSN: 0031-9007

Fischer Th. M., Dhar P., Heinig P. 2006. The viscous drag of spheres and filaments moving in membranes or monolayers, *J. Fluid Mech.* 558 (1) 451-475, ISSN: 0022-1120

Gardel M.L., Valentine M.T., Weitz D.A., 2005, Microrheology. In *Microscale diagnostic techniques*. Brauer K., ed. Springer, ISBN: 978-3-540-23099-1, Berlin.

Gavranovic G.T., Deutsch J.M., Fuller G.G., 2005, Two-dimensional melts: Chains at the air-water interface. *Macromolecules,* 38 (15) 6672-6679, ISSN: 0024-9297

Guo J., Baker G.A., Hillesheim P.C., Dai S., Shaw R.W., Mahurin S.M. 2011. Fluorescence correlation spectroscopy evidence for structural heterogeneity in ionic liquids. *Phys. Chem. Chem. Phys.* 13 (27), 12395-12398, ISSN: 1463-9076

Hasnain I., Donald A.M., 2006, Microrheology characterization of anisotropic materials. *Phys. Rev. E* 73 (3) 031901, ISSN: 1539-3755

Heuf R.F., Swift J.L., Cramb D.T., 2007, Fluorescence correlation spectroscopy using quantum dots: Advances, challenges and opportunities. *Phys. Chem. Chem. Phys.* 9 (16) 1870-1880, ISSN: 1463-9076

Hilles H.M., Ritacco H., Monroy F., Ortega F., Rubio R.G. 2009. Temperature and concentration effects on the equilibrium and dynamic behavior of a Langmuir monolayer: From fluid to gel-like behavior. *Langmuir* 25 (19) 11528-11532, ISSN: 0743-7463

Hughes B.D., Pailthorpe P.A., White L.P. 1981. The translational and rotational drag of a cylinder moving in a membrane. *J. Fluid Mechanics* 110 (1) 349-372, ISSN: 0022-1120

Kahir, A.S., Brady, J.F., 2005, "Microviscoelasticity" of colloidal dispersions, *J. Rheol.*, 49 (6) 1449-1481; ISSN: 0148-6055

Keller M., Schilling J., Sackmann E., 2001, Oscillatory magnetic bead rheometer for complex fluid microrheometry. *Rev. Sci. Instrum.* 72 (9) 3626-3634, ISSN: 0034-6748

Konopka M.C., Weisshaar J.C., 2004, Heterogeneous motion of secretory vesicles in the actin cortex of live cells: 3D tracking to 5-nm accuracy. *J. Phys. Chem. A* 108 (45) 9814-9826, ISSN: 1520-6106

Kralchewski P., Nagayama K., 2001, Particles at fluid interfaces, attachment of colloid particles and proteins to interfaces and formation of two-dimensional arrays. In *Studies in interfacial science*, Vol. 10., Möbius D., Miller R., (Eds.), Elsevier, ISBN: 978-0-444-52180-4, Amsterdam.

Langevin D., 2000, Influence of interfacial rheology on foam and emulsion properties. *Adv. Colloid Interf. Sci.* 88 (1-2) 209-222, ISSN: 0001-8686

Larson R.G., 1999, *The structure and rheology of complex fluids*. Oxford University Press, ISBN: 978-0195121971, New York.

Lee M.H., Lapointe C.P., Reich D.H., Steebe K.J., Leheny R., 2009, Interfacial hydrodynamic drag on nanowires embedded in thin oil films and protein layers, *Langmuir* 25 (14) 7976-7982, ISSN: 0743-7463

Lee M.H., Reich D.H., Steebe K.J., Leheny R.L., 2010, Combined passive and active microrheology study of protein-layer formation at an air-water interface, *Langmuir* 26 (4) 2650-2658, ISSN: 0743-7463

Levine A.J., Lubensky T.C., 2000, One- and two-particle microrheology. *Phys. Rev. Lett.* 85 (8) 1774-1777, ISSN: 0031-9007

Lin B., Rice S.A., Weitz D.A., 1993, Static and dynamic evanescent wave light scattering studies of diblock copolymers adsorbed at the air/water interface. *J. Chem. Phys.,* 99 (10) 8308-8324, ISSN: 0021-9606

Liu J., Gardel M.L., Kroy K., Frey E., Hoffman B.D., Crocker J.C., Bausch A.R., Weitz D.A., 2006, Microrheology probes length scale dependent rheology. *Phys. Rev. Lett.* 96 (11) 118104, ISSN: 0031-9007

MacKintosh F.C., Schmidt C.F., 1999, Microrheology. *Curr. Opinion Colloid Interf. Sci.* 4 (4), 300-307, ISSN: 1359-0294

Madivala B., Fransaer J., Vermant J. 2009. Self-assembly and rheology of ellipsoidal particles at interfaces. *Langmuir* 25 (5) 2718-2728, ISSN: 0743-7463

Maestro A., Guzmán E., Chuliá R., Ortega F., Rubio R.G., Miller R. 2011.a. Fluid to soft-glass transition in a quasi-2D system: Thermodynamic and rheological evidences for a Langmuir monolayer. *Phys. Chem. Chem. Phys.* 13 (20) 9534-9539, ISSN: 1463-9076

Maestro A., Bonales L.J., Ritacco H., Fischer Th.M., Rubio R.G., Ortega, F., 2011.b. Surface rheology: Macro- and microrheology of poly(tert-butyl acrylate) monolayers. *Soft Matter*, in press,ISSN: 1744-683X

Marcus A.H., Lin B., Rice S.A., 1996, Self-diffusion in dilute quasi-two-dimensional hard sphere suspensions: Evanescent wave light scattering and video microscopy studies. *Phys. Rev. E* 53 (2) 1765-1776, ISSN: 1539-3755

Mason T.G., Weitz D.A., 1995, Optical measurements of frequency-dependent linear viscoelastic moduli of complex fluids. *Phys. Rev. Lett*. 74 (7) 1250-1253, ISSN: 0031-9007

Mason Th.G., 2000, Estimating the viscoelastic moduli of complex fluids using the generalized Stokes-Einstein equation. *Rheol. Acta,* 39 (4) 371-378, ISSN: 0035-4511

Miller R., Liggieri L., (Eds.), 2009, *Interfacial rheology.* Brill, ISBN: 9789004175860, Leiden.

Mukhopadhyay A., Granick S., 2001, Micro- and nanorheology, *Curr. Opinion Colloid Interf. Sci.* 6 (5-6),423-429, ISSN: 1359-0294

Muñoz M.G., Monroy, F., Ortega F., Rubio R.G., Langevin D., 2000, Monolayers of symmetric triblock copolymers at the air-water interface. 2. Adsorption kinetics. *Langmuir* 16 (3) 1094-1101, ISSN: 0743-7463

Oppong F.K., de Bruyn J.R., 2010, Microrheology and dynamics of an associative polymer, *Eur. Phys. J. E* 31 (1) 25-35, ISSN: 1292-8941

Ou-Yang H.D., Wei M.T., 2010, Complex fluids: Probing mechanical properties of biological systems with optical tweezers, *Ann. Rev. Phys. Chem.*, 61, 421-440, ISSN: 0066-426X

Pan W., Filobelo L., Phan N.D.Q., Galkin O., Uzunova V.V., Vekilov P.G., 2009, Viscoelasticity in homogeneous protein solutions, *Phys. Rev. Lett.* 102 (5) 058101, ISSN: 0031-9007

Paunov V.N. 2003. Novel Method for Determining the Three-Phase Contact Angle of Colloid Particles Adsorbed at Air−Water and Oil−Water Interfaces. *Langmuir* 19 (19) 7970–7976, ISSN: 0743-7463

Prasad V., Weeks E.R., 2009, Two-dimensional to three-dimensional transition in soap films demonstrated by microrheology, *Phys. Rev. Lett.* 102 (17) 178302, ISSN: 0031-9007

Resnick A., 2003, Use of optical tweezers for colloid science, *J. Colloid Interf. Sci.* 262 (1) 55-59, ISSN: 0021-9797

Reynaert S., Moldenaers P., Vermant J. 2007. Interfacial rheology of stable and weakly aggregated two-dimensional suspensions. *Phys. Chem. Chem. Phys.* 9 (48) 6463-6475, ISSN: 1463-9076

Reynaert S., Brooks C.F., Moldanaers P., Vermant J., Fuller G.G., 2008. Analysis of the magnetic rod interfacial stress rheometer. 52 (1), 261-285, ISSN: 0148-6055

Riande E., Díaz-Calleja R., Prolongo M.G., Masegosa R.M., Salom C., 2000, *Polymer viscoelasticity. Stress and strain in practice*. Marcel Dekker, ISBN: 0-8247-7904-5, New York.

Ries J., Schwille P., 2008, New concepts for fluorescence correlation spectroscopy on membranes. *Phys. Chem. Chem. Phys.* 10 (24) 3487-3497, ISSN: 1463-9076

Riegler R., Elson E.S., 2001, *Fluorescence correlation spectroscopy: Theory and applications.* Springer-Verlag, ISBN; 978-3540674337, Berlin.

Saffman P-G., Delbrück M. 1975. Brownian Motion in Biological Membranes. *Proc. Nat. Acad. Sci. USA* 72 (8) 3111-3113, ISSN: 1091-6490

Saxton M.J., Jacobson K., 1997, Single-particle tracking: Applications to membrane dynamics. *Annu. Rev. Biophys. Biomol Struct.* 26 (1) 373-399, ISSN: 1056-8700

Schmidt F.G., Hinner B., Sackmann E., 2000, Microrheometry underestimates the values of the viscoelastic moduli in measurements on F-actin solutions compared to macrorheometry, *Phys. Rev. E* 61 (5) 5646-5652, ISSN: 1539-3755

Sickert M., Rondelez F. 2003. Shear viscosity of Langmuir monolayers in the low density limit. *Phys. Rev. Lett.* 90 (12) 126104, ISSN: 0031-9007

Sickert M., Rondelez F., Stone H.A. 2007. Single-particle Brownian dynamics for characterizing the rheology of fluid Langmuir monolayers. *Eur. Phys. Lett.* 79 (6) 66005, ISSN: 0295-5075

Squires T.M., 2008, Nonlinear microrheology: Bulk stresses versus direct interactions. *Langmuir* 24 (4) 1147-1159, ISSN: 0743-7463

Squires T.M., Mason Th.G., 2010, Fluid mechanics of microrheology, *Ann. Rev. Fluid Mechanics*, 42 (1) 413-438, ISSN: 0066-4189

Steffen P., Heinig P., Wurlitzer S., Khattari Z., Fischer Th.M., 2001, The translational and rotational drag on Langmuir monolayer domains, *J. Chem. Phys.* 115 (2) 994-997, ISSN: 0021-9606

Stone H., Adjari A. 1998. Hydrodynamics of particles embedded in a flat surfactant layer overlying a subphase of finite depth. *J. Fluid Mech.* 369 (1) 151-173, ISSN: 0022-1120

Tassieri M., Gibson G.M., Evans R.M.L., Yao A.M., Warren R., Padgett M.J., Cooper J.M., 2010, Optical tweezers. Broadband microrheology, *Phys. Rev. E* 81 (2) 026308, ISSN: 1539-3755

Vincent R.R., Pinder D.N., Hemar Y., Williams M.A.K., 2007, Microrheological studies reveal semiflexible networks in gels of a ubiquitous cell wall polysaccharide. *Phys. Rev. E* 76 (3) 031909, ISSN: 1539-3755

Waigh T.A., 2005, Microrheology of complex fluids. *Rep. Prog. Phys.* 68 (3) 685-742, ISSN: 0034-4885

Wilson L.G., Poon W.C.K., 2011, Small-world rheology: An introduction to probe-based active microrheology, *Phys. Chem. Chem. Phys.* 13 (22) 10617-10630, ISSN: 1463-9076

Winkler R.G., 2007, Diffusion and segmental dynamics of rodlike molecules by fluorescence correlation spectroscopy. *J. Chem. Phys.*127 (5) 054904, ISSN: 0021-9606

Wöll D., Braeken E., Deres A., de Schryver F.C., Uji-I H., Hofkens J., 2009. Polymers and single molecule fluorescence spectroscopy, what can we learn? *Chem. Soc. Rev.* 38 (2), 313-328, ISSN: 0306-0012

Wu J., Dai L.L., 2006, One-particle microrheology at liquid-liquid interfaces. *Appl. Phys. Lett.,* 89 (9) 094107, ISSN: 0003-6951

Yoon Y-Z., Kotar J., Yoon G., Cicuta P., 2008, The nonlinear mechanical response of the red blood cell. *Phys. Biol.* 5 (3) 036007, ISSN: 1478-3975

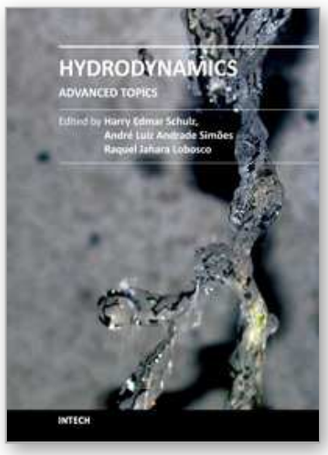

Hydrodynamics - Advanced Topics

Edited by Prof. Harry Schulz

ISBN 978-953-307-596-9

Hard cover, 442 pages

Publisher InTech

Published online 22, December, 2011

Published in print edition December, 2011

The phenomena related to the flow of fluids are generally complex, and difficult to quantify. New approaches - considering points of view still not explored - may introduce useful tools in the study of Hydrodynamics and the related transport phenomena. The details of the flows and the properties of the fluids must be considered on a very small scale perspective. Consequently, new concepts and tools are generated to better describe the fluids and their properties. This volume presents conclusions about advanced topics of calculated and observed flows. It contains eighteen chapters, organized in five sections: 1) Mathematical Models in Fluid Mechanics, 2) Biological Applications and Biohydrodynamics, 3) Detailed Experimental Analyses of Fluids and Flows, 4) Radiation-, Electro-, Magnetohydrodynamics, and Magnetorheology, 5) Special Topics on Simulations and Experimental Data. These chapters present new points of view about methods and tools used in Hydrodynamics.

InTech Europe

University Campus STeP Ri
Slavka Krautzeka 83/A
51000 Rijeka, Croatia
Phone: +385 (51) 770 447
Fax: +385 (51) 686 166
www.intechopen.com

InTech China

Unit 405, Office Block, Hotel Equatorial Shanghai
No.65, Yan An Road (West), Shanghai, 200040, China
中国上海市延安西路65号上海国际贵都大饭店办公楼405单元
Phone: +86-21-62489820
Fax: +86-21-62489821

IntechOpen